Supplemental Material

Supplemental Figure Legends:

Supplemental Figure 1: ISHAGE enumeration of canine HPCs (CD34+ $CD45_{dim}$ VEGFR2- progenitor cells)

A. After incubation of cells with fluorophore-conjugated antibodies to CD45 and CD34, data are displayed as a dotplot of side scatter (SSC) vs. CD45 fluorescence. All CD45 positive events are gated in a region R1.

B. Data in R1 is displayed as a dotplot of side scatter vs. CD34 fluorescence. A CD34 positive cluster of low side scatter should be apparent which is gated R2.

C. Data from R2 are displayed in a dotplot SSC vs CD45 fluorescence. The CD45-dim population is gated R3.

D. Returning to the SSC vs CD45 dotplot and switching off all gates again, a new gate R4 is created around the homogenous, CD45 positive and low side scatter lymphocyte population.

E. R4 is displayed as a dotplot of side scatter vs. forward scatter. This shows the phenotypic characteristics of the lymphocytes and blasts, which are similar to those of hematopoetic precursors. A region R5 is created to set the boundaries of these defining phenotypic features.

F. Contents of R1x R2 x R3 are displayed as in E. All events outside R5 are excluded from the final count, which represents the number of CD34+ $CD45_{dim}$ positive cells per 60,000 events. These cells are uniformly VEGFR2 negative.

Supplemental Figure 2: Enumeration of canine CD34+ CD45- VEGFR2+ progenitor cells (EPCs)

A. After incubation of cells with fluorophore-conjugated antibodies to CD45 and CD34, data are displayed as a dotplot of side scatter (SSC) vs. CD45 fluorescence. All CD45 negative events are gated in a region R1.

B. Data in R1 is displayed as a dotplot of side scatter vs. CD34 fluorescence. A CD34 positive cluster of low side scatter should be apparent which is gated R2.

C. Data from R2 are displayed in a dotplot SSC vs CD45 fluorescence. The CD34+ CD45-negative population is visible by gating on R1 * R2.

D. In a dotplot of SSC vs VEGFR2 a new gate R3 is created around all VEGFR2+ events.

E. In the same dotplot, CD34+ CD45- VEGFR2+ events are demonstrated by gating on R1 * R2 * R3. Contents of R1x R2 x R3 are displayed in a dotplot of SSC vs. FSC (forward scatter). The low side scatter, low forward scatter nature of these cells is apparent.

Supplemental Figure 3: A: Hematopoietic (HPC) and B: endothelial progenitor cell (EPC) counts in a canine pacing model of LV dysfunction, expressed as absolute counts. Cells were enumerated from paced dogs at baseline and at 10 days, compared using a Wilcoxon signed-rank test.

Supplemental Figure 4: Neurohumoral correlates of progenitor cell counts: Spearman Rank correlation (ρ) of change in progenitor cell counts from paced dogs over 10 days compared with plasma aldosterone level (A), canine B-type natriuretic peptide (cBNP)

(B) levels, and canine atrial natriuretic peptide levels (ANP) (C) at 10 days. For clarity, correlations are shown in a linear fashion.

Supplemental Figure 5. Immunodetection of VEGFR2 expression in canine cells. **A**. Canine aortic endothelial cells (Cell applications, Inc.) stained with control IgG. Hoechst counterstain depicts nuclei. **B**. Canine aortic endothelial cells stained with anti-VEGFR2 and Hoechst. **C**. FACS analysis of canine endothelial cells using IgG and the anti-VEGFR2 antibodies

Supplemental Figure 1

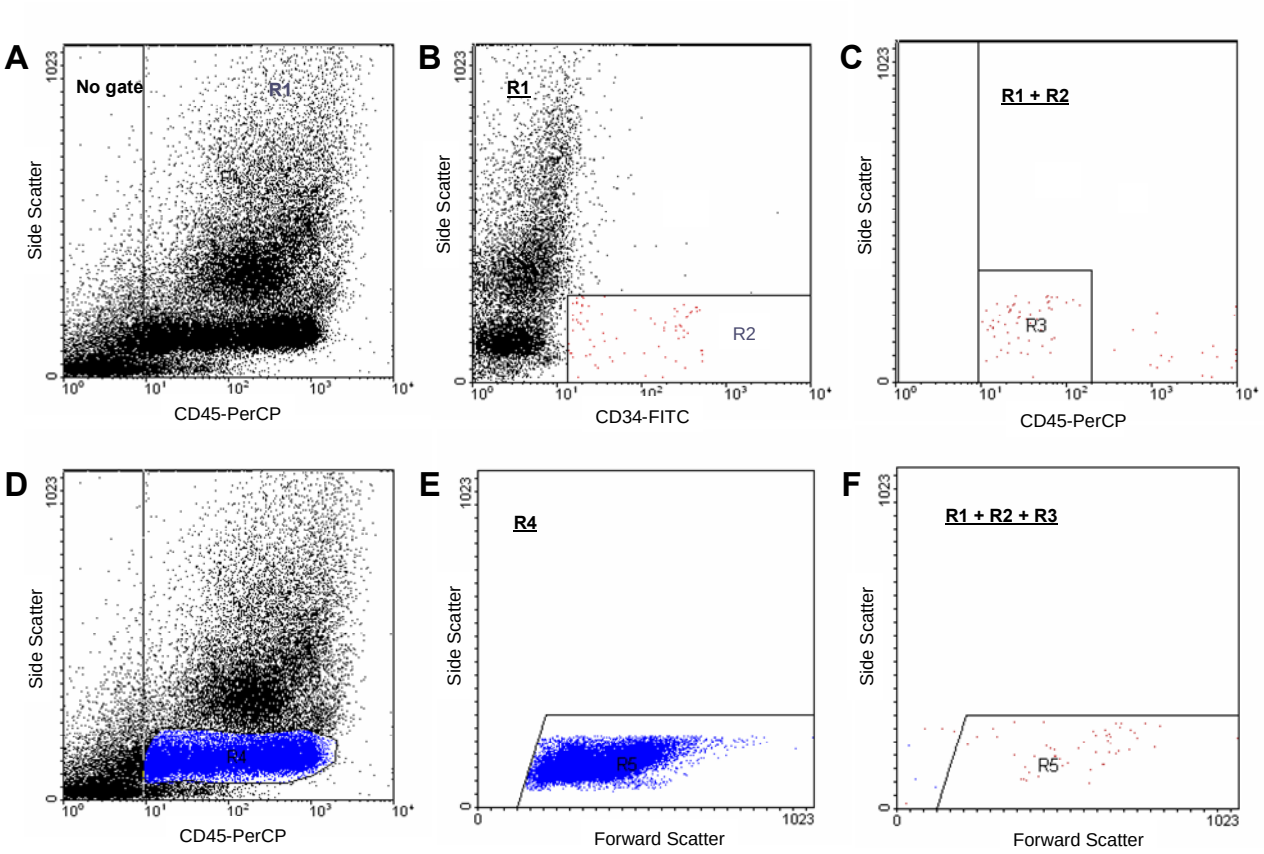

Supplemental Figure 2

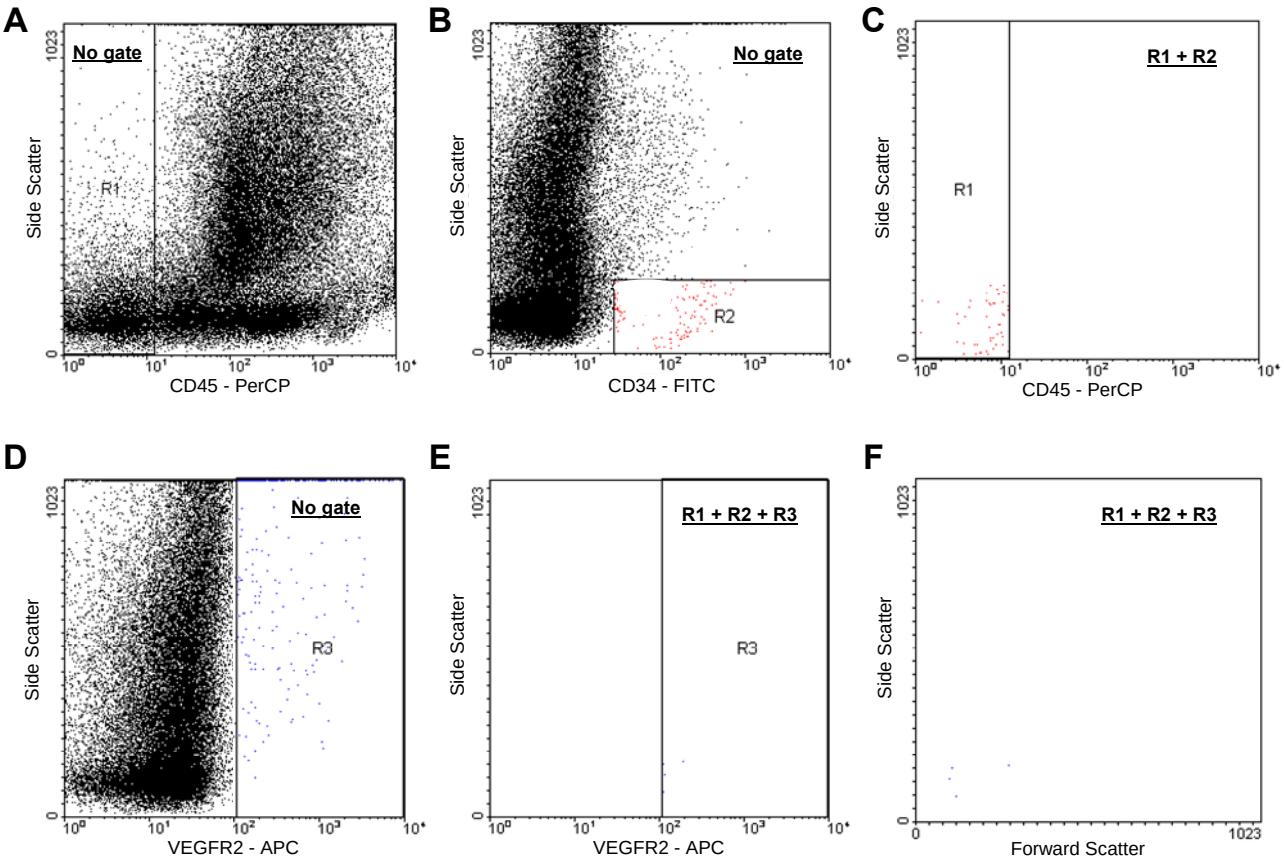

Supplemental Figure 3

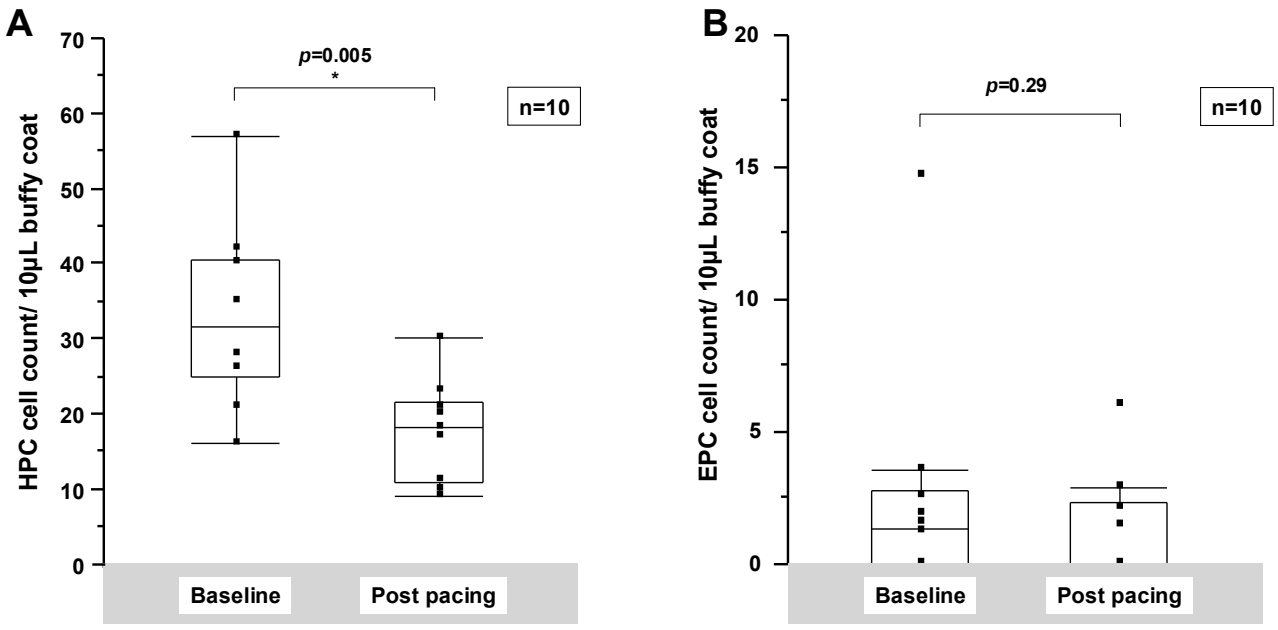

Supplemental Figure 4

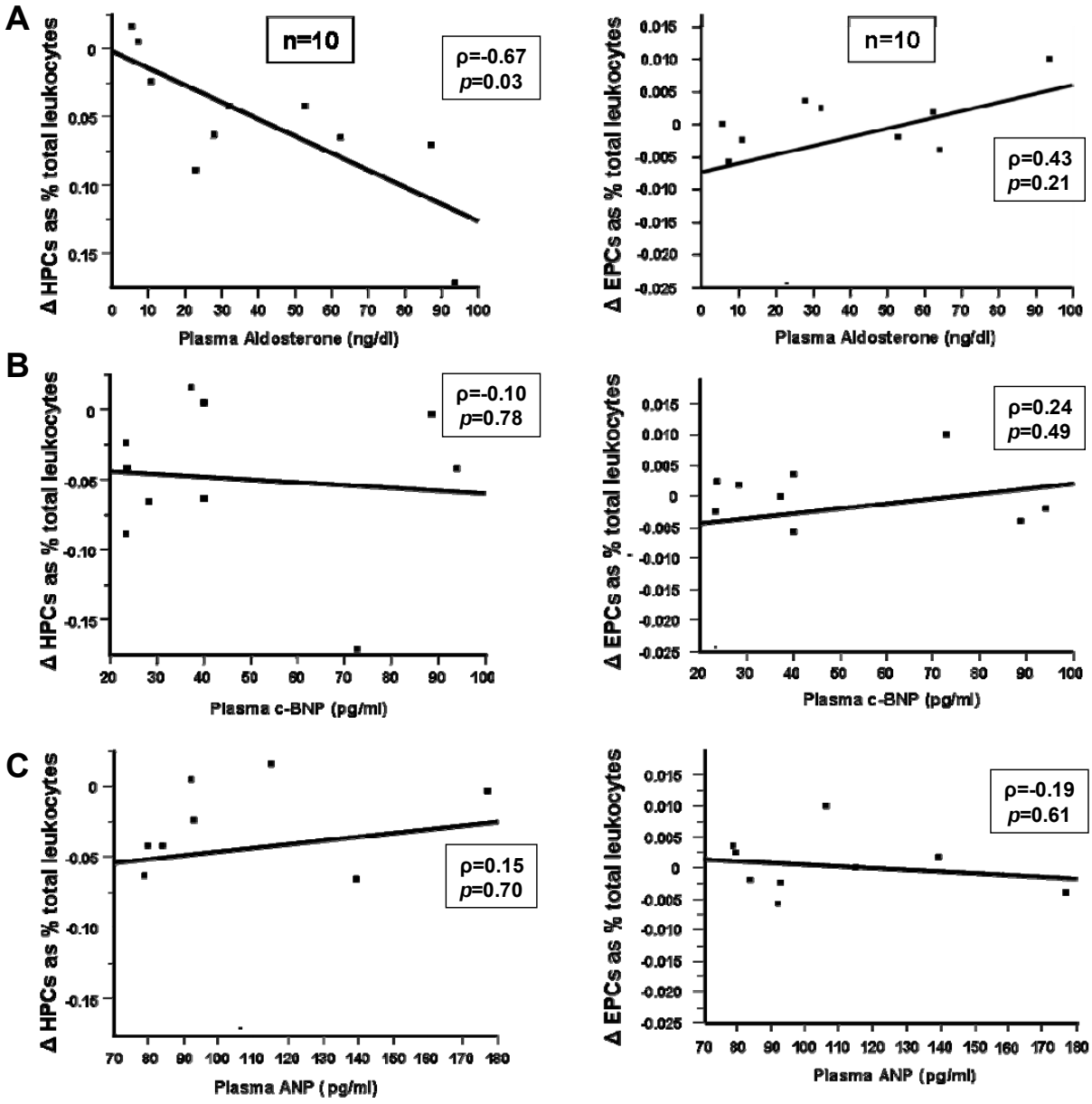

Supplemental Figure 5